Materials Research Express

PAPER

Effect of flame spray deposition parameters on the microstructure, microhardness and corrosion resistance of FeNbC coatings on AISI 1020 steel

To cite this article: I Bonetti *et al* 2019 *Mater. Res. Express* **6** 086530

Materials Research Express

PAPER

Effect of flame spray deposition parameters on the microstructure, microhardness and corrosion resistance of FeNbC coatings on AISI 1020 steel

RECEIVED
26 November 2018

REVISED
21 March 2019

ACCEPTED FOR PUBLICATION
9 April 2019

PUBLISHED
8 May 2019

I Bonetti[1], E A dos S de[2], C E da Costa[2], R S C Paredes[3], G B Sucharski[3], E M da Costa[4], E Franco[2] and J C G Milan[2]

[1] Instituto Federal de Santa Catarina–IFSC, Rua Pavão, 1337, Joinville, SC, Brasil
[2] Universidade do Estado de Santa Catarina—UDESC, Campus Universitário Prof. Avelino Marcante—Rua Paulo Malschitzki, 200, Joinville, SC, Brasil
[3] Universidade Federal do Paraná–UFPR–Centro Politécnico, Av. Cel. Francisco H. dos Santos, 100—Jardim das Américas, Curitiba, PR, Brasil
[4] Pontifícia Universidade Católica do Rio Grande do Sul–PUC RS, Escola Politécnica, Av. Ipiranga, 6681—Partenon, Porto Alegre, RS, Brasil

E-mail: ivandro.bonetti@gmail.com

Keywords: coatings, niobium, flame spraying, cermet FeNbC

Abstract

The present study aimed to produce and characterize FeNbC coatings deposited on AISI 1020 steel using flame spray process (FS) evaluating the influence of powder granulometry, standoff distance, powder feed rate and substrate preheating. FS process parameters variations produce coatings with different properties. Taguchi experimental design based in the L9 orthogonal array and ANOVA statistical analysis were performed. Coating morphology was evaluated using scanning electron microscopy (SEM) and energy dispersive spectroscopy (EDS), the present phases were identified by x-ray diffraction (XRD). Coatings microhardness was evaluated using Knoop hardness test. The coatings corrosion resistance was measured through monitoring the open circuit potential and potenciodynamic polarization in 3.5% NaCl solution. The results indicate that coatings with microhardness average of 1084 $HK_{0.3}$ and dispersion of the measured values were associated with heterogeneity and interlamellar oxides formed in the microstructure. All control factors investigated showed significant influence on microhardness. Substrate preheating was the most important factor, followed by the powder granulometry; powder feed rate and standoff distance. The FeNbC coating presented a reduction in the substrate corrosion rate, but the presence of defects in the microstructure, such as porosities, voids and cracks compromised the barrier effects of these coatings.

1. Introduction

The recent discovery of petroleum in the deep-sea of Brazilian coast has aroused the scientific interest for the development of wear-resistant and corrosion-resistant coatings that exhibit environmentally favorable behavior. In the 1990's and 2000's, the availability and price of niobium turned the application prohibitive; however, the use of this material as a microligant to steels significantly increased its demand. Currently, the use of ferroniobium alloys in pipe coatings and as a microconstituent in steels for structural applications accounts for a sales volume of 85000 tons per year [1]. Therefore, the use of niobium as protective coating against wear and corrosion on carbon steel substrate is an economical alternative for several practical situations [2]. The application of thermal spraying coatings of niobium carbide on the steel substrate has emerged as an alternative to other coating processes like welding, cold or solid welding [3–5].

The main application of niobium is the ferroniobium alloy covering about 90% of the consumer market [6]. Ferroniobium is widely employed as an additive in the development of high temperature wear resistant alloy steel with typical additions in the range of 0.04% by weight. These steels are generally used in the construction of

oil and gas pipelines on offshore oil drilling rigs. In the automotive industry, they are employed in structural components that require high mechanical strength such as wheels and chassis. In the railway industry, they are applied in the manufacture of rails in curves and deviation where there is more intense wear [7]. Niobium carbide precipitation in a metal matrix generates surface hardening and increases corrosion and oxidation resistance at high temperatures leading to an increase in the useful life of components making them suitable for industrial applications [8].

Different manufacturing processes can be employed in order to obtain corrosion-resistant coatings based on niobium carbide, for example CVD, PVD and electrodeposition [9–11]. However, thermal spraying is an option that allows advantages such as high production rate, lower investment and operating costs, greater versatility and lower environmental impact.

The cost of wear and corrosion is estimated to be around 3 to 5 percent of developed nations' GDP. These failure mechanisms result in degradation, shortening the life of many components of industrial systems [12]. Thus thermal spraying coating presents technical interest as a barrier to minimize the effect of wear and corrosion.

Thermal spraying is a deposition process in which molten, semi-solid or solid particles are sprayed onto a substrate with a certain level of kinetic and thermal energy and are then mechanically anchored forming a refined multilayer lamellar structure [13]. Spraying processes can be classified into two groups according to the energy source used to heat and melt the material to be deposited. There are combustion processes: flame [14], plasma [15], high velocity oxy-fuel (HVOF) [16], cold spraying [17] and D-gun [18], and electric arc processes: atmospheric plasma spraying (APS) [19] plasma transferred arc spraying (PTA) [20, 21] electric spraying (ES) [22].

Flame spraying was chosen because it is a simple process, economically viable considering the production of a small number of samples and because it produces thicker coatings using different types of metallic, ceramic, composite or polymer materials [23, 24]. The flame spraying process is characterized by lower particle acceleration, lower deposition temperature and poor control of the surrounding atmosphere, which may lead to the formation of a greater amount of porosity, interlamellar cracking, oxides formation and low cohesion between the splats. The porosity in the coating depends on factors related to the starting material, such as particle size and especially the melting temperature. The melting temperature of the niobium carbide (Tm $=$ 3600 °C) is higher than the iron melting temperature (Tm $=$ 1538 °C), such a difference can influence the formation of cracks and porosity in the layer. In the deposition of powder material by flame spraying the main process parameters are related to: particle size, temperature and speed, angle and feed rate, spraying distance and substrate preheating temperature [25]. The objective of this work is to evaluate a coating based on FeNbC characterizing the behavior of corrosion resistance, microstructure and microhardness of the cross-section according to the variation of thermal spraying process operational parameters

2. Materials and methods

The FeNbC powder used was reduced in size by milling (received from the supplier with particle size greater than 1 mm). The procedure for preparation of the spraying powder was carried out in a planetary mill using the Pulverisette model from Fritsch manufacturer and SAE/AISI 52100 steel balls, the ratio ball/powder used was 3:1, grinding time of 20 min at 300 rpm. In order to avoid oxidation of FeNbC the grinding was carried out in argon atmosphere with a pressure of 3 kgf mm^{-2}.

The material used in the deposition was separated into different volumetric fractions by mechanical sieving according to ASTM C 136-01, particles smaller than 53 μm (-53 μm), smaller than 75 μm (-75 μm) and the grain size range between 53 and 75 ($-75 + 53$ μm). The particles size used in the spraying were measured by laser diffraction using a Shimadzu SALD 220 equipment. Chemical composition is shown in table 1. Before spraying the coating, the powder was kept in a muffle furnace at 120 °C for 30 min to eliminate humidity and possible contaminants that could impair feedability during the spraying process.

Taguchi´s methodology was used to define the experimental planning, which allows obtaining information using a smaller number of experiments, thus reducing effort, cost and time. To evaluate the response signal, triplicates of the samples were used in an orthogonal array L9, in which it was possible to study 4 factors with 3 levels presented in the orthogonal matrix described in table 2.

Oxyacetylene flame spray process was selected because of its high flame temperature. The spray gun was maintained perpendicular to the substrate during deposition to ensure lowest porosity and interlamellar oxides intensity in the coating [26]. The thickness of the coating was kept uniform since the samples were held fixed in the setting device and the spray gun was moved within a predetermined spraying distance and at constant speed. The coating thickness is dependent on the number of passes performed in the deposition process [27] . Five

Table 1. FeNbC Chemical composition (wt%).

Nb	Fe	C	Al	Ti (ppm)	Si	Ta	Pb	S
40.2	43.3	6.51	3.92	489	0.80	<0.10	<0.10	0.03

Table 2. Set of factors and levels used in this study.

	Level		
Control factor	1	2	3
Granulometry (μm)	-53	-75	$-75 + 53$
Standoff distance (mm)	150	200	250
Powder feed rate (g.min^{-1})	40	50	60
Substrate preheating (°C)	50	150	250

Table 3. Parameters used in thermal spray coatings by FS.

Oxygen pressure	0.276 MPa
Oxygen flow	2.260 Nm^3 h^{-1}
Acetylene pressure	0.103 MPa
Acetylene flow	1.133 Nm^3 h^{-1}
Carrier gas pressure (Argon)	0.338 MPa
Carrier gas flow (Argon)	0.283 Nm^3 h^{-1}
Air pressure	0.100 Mpa

consecutive passes were taken to ensure that the thickness of the entire surface of the specimen is less than 250 μm, according ASTM C 633-93.

The coating was obtained in a flame spray system using 5 MPE powder feed model with 6P-II pistol from the manufacturer Sulzer Metco. The process parameters are shown in table 3.

Oxidizing flame was used with a combustion rate of 2:1 (oxygen:acetylene) assuring the adequate temperature in the spraying process. This rate guarantees the complete combustion of the acetylene. Inefficient combustion could generate a greater amount of unmelted particles and inclusions of interlamellar oxides, which would impair the properties of the coating. According to Tucker [28], the stoichiometry of gases used in the combustion also exerts influence on the particles thermal energy that reach the substrate, and thus define the mechanical properties of the coating.

2.1. Substrate preparation

The substrate used in this work was AISI 1020 steel. Prior to deposition, the substrate was submitted to ultrasonic cleaning and abrasive blasting. Initially they were cleaned in acetone in an ultrasonic bath for 5 min, followed by abrasive blasting with brown aluminum oxide with R 20 AISI/FEPA grading, with a working pressure of 0.414 MPa, a spraying distance of 150 mm and a deposition angle of 90°. Thus, the average roughness Ra obtained was 7.86 μm. The triplicates of the samples used for characterization were obtained from the section of specimens from a substrate measuring 50 $\times$ 25 $\times$ 1.25 mm. The wettability between particles and substrate is an important parameter that allows the mechanical anchoring, and consequently the adhesion of the coating. One way to change the wettability is to preheat the substrate [29, 30], considering this factor, the influence of preheating was determined by the evaluation of coating adhesion strength. The literature indicates that adhesion/cohesion of coatings obtained with preheated substrate is better than the coatings adhesion obtained without preheating [31].

2.2. Characterization methods

X-ray diffraction (Shimadzu XRD-7000 equipment) identified the phases in FeNbC powder and coated samples. Cu-Kα target radiation was used with 2θ angle ranging from 20 to 120°. The crystalline phases were identified using PANalytical X'Pert HighScore Plus software, v3.0 and with the JCPDS index database.

Coating cross-section morphology was investigated using scanning electron microscopy (SEM) with a JEOL-JSM 6107 equipment. Mapping and punctual analysis of semi-quantitative chemical composition was performed by energy dispersive spectroscopy (EDS).

The microhardness was measured by 15 indentations in the cross-section of each coating experimental condition using a Shimadzu HVM-2T microdurometer. A Knoop indenter was used with load of 300 gf for 10 s and distance between indentations of 3 diagonals.

Electrochemical measurements of polarization resistance were carried out using Autolab potentiostat (PGSTAT 302 N), in order to evaluate the performance of FeNbC coatings in terms of corrosion protection to steel. Polarization tests were conducted at room temperature using a classical three-electrode configuration: a saturated calomel electrode (SCE) as reference electrode, platinum wire as counter electrode and a working electrode formed by the sample being tested. The potentiodynamic polarization curves were obtained in a 3.5% NaCl solution, using a scan rate of 1 mV s^{-1} and potential range of −300 to +300 mV in relation to open circuit potential (OCP). The sample was left at open circuit potentials for 1 h before acquire polarization curves. The electrochemical parameters were obtained by Tafel extrapolation method using Nova-Autolab software version 1.0.

3. Results and discussion

3.1. Microstructural analysis of powder and coating

The morphology of the FeNbC powder used in the spraying process is shown in figure 1. Powder underwent an intense fracture mechanism and welding of particles during the high energy milling process, promoting an irregular and polygonal shape. The efficiency of the spraying process can be affected by the properties of the powder, especially the particle size. However, even with a great variability in particle size after milling, as shown in figure 1, the powder showed fluidity during the spraying process. No clogging was recorded in the hoses leading the powder from the feeder to the gun. The deficient fluidity would result in a fluctuation of the powder feed, causing the formation of a heterogeneous microstructure with many defects. Large difference in particle size may represent a problem in the spraying process. Large particles have high mass, and impair the promotion of the adequate acceleration in deposition, otherwise powder composed of reduced size particles can cause clogging in the spraying supply system [32].

The particle size of the FeNbC powder obtained by the high energy milling comprised the range from 53 μm to 75 μm. The particle size analysis by laser diffraction in the powder in which the largest particle had a diameter of 53 μm demonstrated that D90 of 31.853 μm, whereas the powder which had the largest particle size of 75 μm was the D90 of 44.850 μm.

The frequency distribution of the particle size, in figure 2 (a), shows that about 27% of the powder with particle size −53 μm had a size ranging from 17.222 to 74.008 μm. Although the grinding process using the ABNT 270 sieve allows the separation of particles with sizes smaller than 53 μm, it is possible that some larger particle were not retained in the sieve due to a possible deformation of the sieve mesh. However, laser diffraction analysis showed that only 0.5% of the volume of the sample material had a particle size above 53 μm. Figure 2(b) indicates that approximately 38% of the particles had a size ranging from 21.210 to 82.131 μm. However, laser diffraction data indicated that 0.13% of the sample volume had a size greater than 75 μm.

The heterogeneity of the coating microstructure typically found in thermal spraying deposition is shown in figure 3(a). A higher magnification of coating cross-section indicated by the dashed line is shown in figure 3(b), where splats are observed parallel to the substrate surface and some porosity regions formed during the cooling process. In several thermal spraying methods the molten or semi-molten particle of the feedstock is accelerated against a substrate, they deform during impact and anchor mechanically on the irregular surface, thereafter on each previously solidified layer, thus giving rise to a multilayer coating with lamellar structure [28, 33]. Unmelted particles and interlamellar cracks are also observed, indicating an inefficient metallurgical bond. The presence of unmelted particles in the coating possibly influenced the formation of cracks and porosities.

The formation of voids and porosity in the thermal spraying coating inevitably occurs at higher or lower level according to the process type. The porosity level found in the coating is associated to the process parameters employed, especially flame temperature, particle velocity, spraying distance [34] and the time interval in which the particles are exposed to the process temperature. Figure 3(a) shows the presence of voids and porosity near the substrate/coating interface, according to Mellali *et al* [35] the first layer deposited in the spraying process is strongly influenced by the substrate preheating. Substrate shown in figure 3(a) was preheated at 250 °C.

The semi quantitative analysis performed by EDS showed the presence of Fe, Nb and Al atoms, as can be observed in figure 4. The presence of aluminum is associated with the alumino-carbothermic reduction process used to obtain FeNbC [36]. Oxygen is also observed, due to the oxidation caused by the particles heating in the spraying process. Other chemical elements were not detected suggesting that there was no contamination during the high energy milling to which the material was submitted [37], neither contamination due to the spraying process.

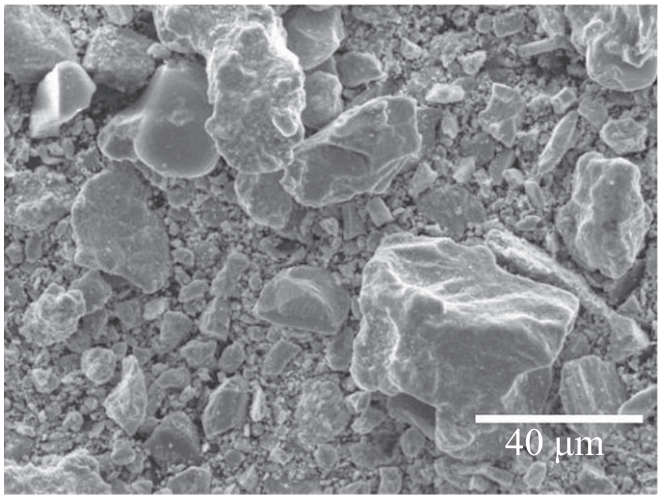

Figure 1. FeNbC powder morphology.

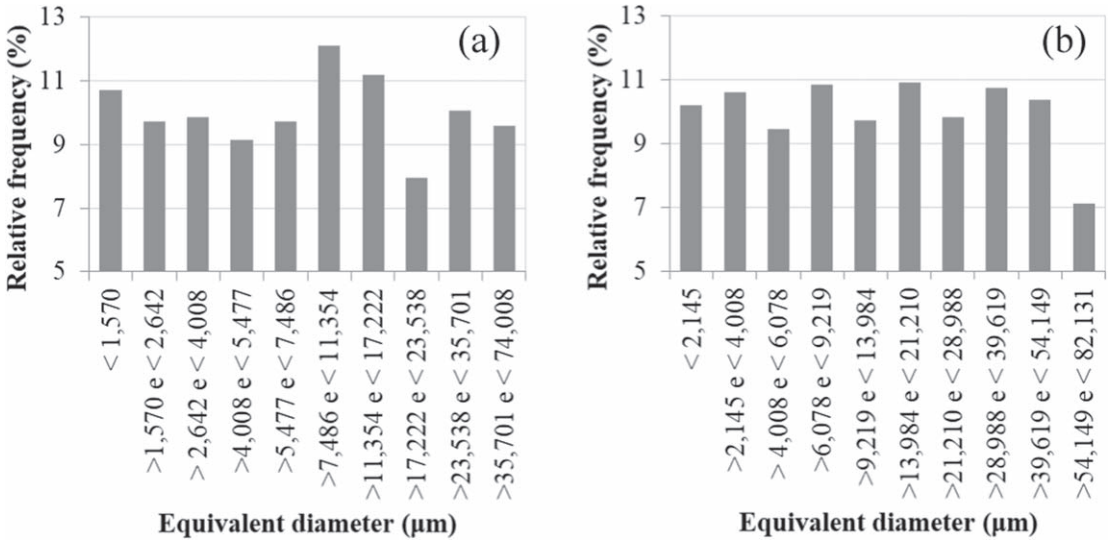

Figure 2. Histogram of frequency distributions of particle size of FeNbC powder. (a) 53 μm, (b) 75 μm.

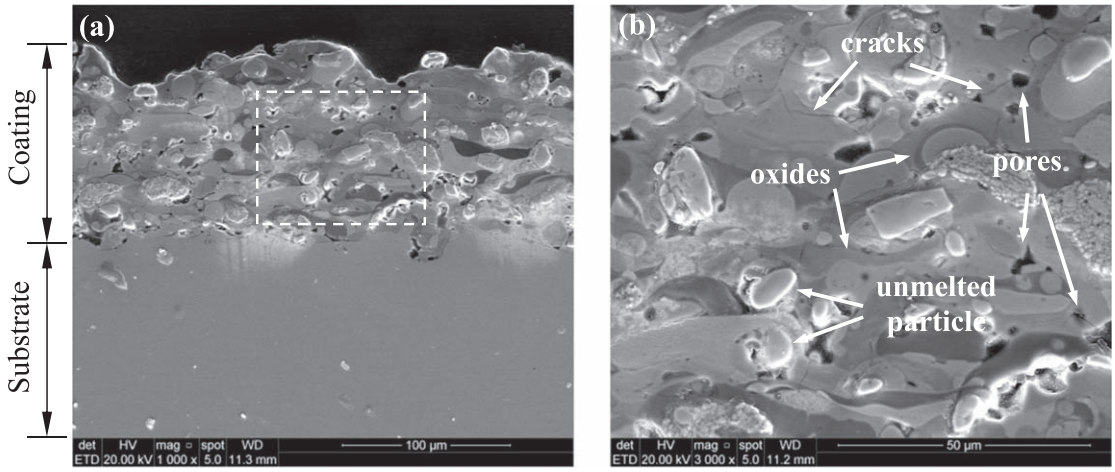

Figure 3. Cross section of steel coated with FeNbC. (a) Highlight for the coating/substrate interface. (b) Major magnification of lamellar and heterogeneous structure of the coating. SEM.

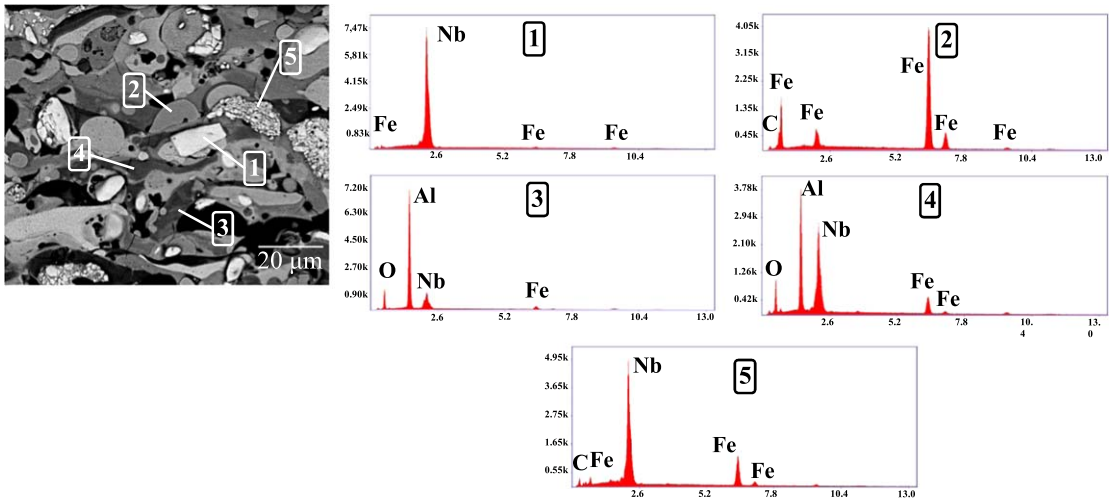

Figure 4. Microstructural analysis by EDS in the coating obtained by backscattered electron image.

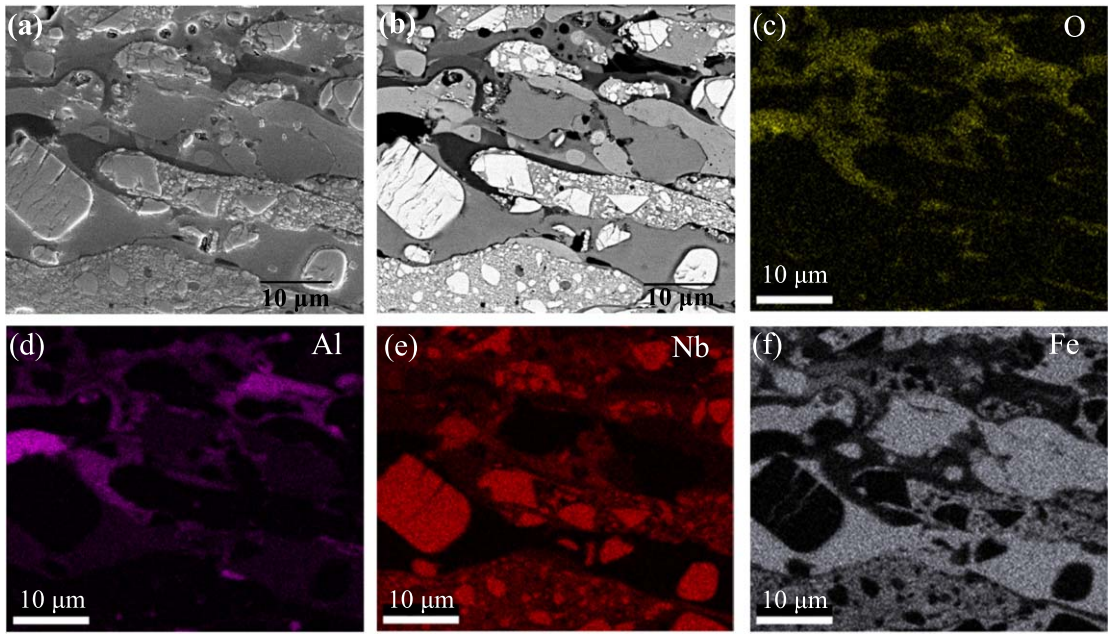

Figure 5. Steel´s cross-section coated with FeNbC: (a) image obtained by secondary electrons, (b) image obtained by backscattered electrons, (c) image mapping O element, (d) image mapping Al element, (e) image mapping Nb element, (f) image mapping Fe element.

EDS analysis identified that region 1 in figure 4 presented a high concentration of Nb corresponding to the NbC phase. The polygonal morphology was typically reported in papers that addressed the topic [4, 38], and the existence of this phase was also identified by XRD. Region 2 shows the presence of iron rich phase, which was also identified by XRD. Regions 3 and 4 show a darker gray shade typically observed in coating micrographs obtained by thermal spraying, chemical analysis identified a high amount of oxygen atoms suggesting that such phases could be oxides formed during the spraying process. Oxide formation can occur in the heated particle during the in-flight to the substrate, as well as after impact during splat cooling, and on the surface of the coating between two sequential deposition passes. The formation of oxides in interlamellar positions depends on the spraying parameters, the presence of oxygen in the deposition system or in the control atmosphere, particle temperature, as well as the physicochemical properties of the powder [39]. Region 5 is characterized by smaller particles of NbC dispersed in the Fe matrix.

The chemical mapping shown in figure 5 identifies oxides regions. The dark gray interlamellar regions in figure 5(b) are oxides phases generated from the spraying, which can be seen in figure 5(c) and the lighter regions

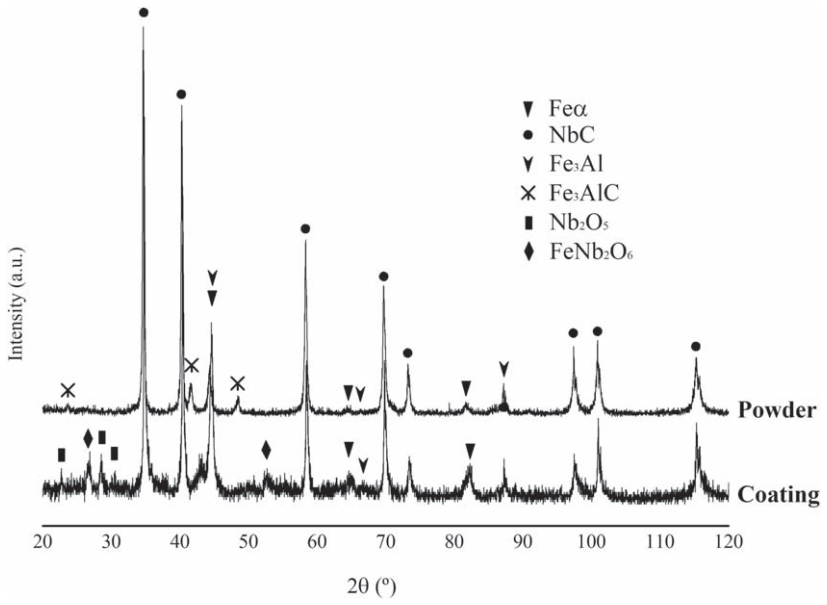

Figure 6. X-ray diffractograms of FeNbC powder and coating.

are sites rich in Nb, while the light gray regions are Fe-rich lamellae, which can be observed in figures 5(e) and (f), respectively. It was also possible to identify porosity regions formed inside the lamellae.

XRD spectrum of FeNbC powder and coating obtained by thermal spraying are shown in figure 6. The diffraction analysis of the powder indicates the presence of NbC, Feα, Fe_3Al, Fe_3AlC phases. The last two phases could be originated during the obtaining of FeNbC by alumino-carbothermic reduction process [36]. Figure 6 does not present other phases suggesting that there was no contamination by the jar material in high energy milling, so the integrity of chemical composition of the material supplied after milling was maintained.

Phases presented in the powder were maintained in the coating diffractogram, as observed in figure 6. Oxide phases were also observed, and identified by EDS. In the thermal spraying process, the presence of free oxygen in the atmosphere associated with the flame temperature makes the formation of oxides in the coating unavoidable. Incrustation of oxides in interlamellar positions can affect the cohesive behavior of the particles and consequently affect the coating wear resistance. In some cases, the presence of oxides increases the microhardness and wear resistance of the layer, but reduces its ductility and impact resistance [40]. The amount of oxides formed in the coating depends on the process parameters employed and the reactivity of the powder used in the spraying [39].

3.2. Microhardness

The coating microhardness was high due to the presence of oxides formed in the thermal spraying process, as shown in figure 6, as well as by the presence of unmelted particles [41], which were observed in the coating obtained in this study. The dispersion of the coating microhardness measured values is associated with the presence of defects, such as porosity and interlamellar cracks as reported by Mao *et al* [42]. Contrary to what was pointed out in the study Yu *et al* [43], it is worth mentioning that in this work the presence of cracks around the indentation region was not observed, as well as at the indentation vicinity, which indicates that the matrix ductile behavior did not contribute to the nucleation and propagation of cracks. Fact that could influence the result obtained for the coating microhardness.

Figure 7 shows the results of microhardness measurement. The indentations were performed only in the cross-section of the coating, in which were observed random differences of microhardness, without the presence of discrepant points and with constant tendency.

The variance analysis indicated that all control factors influence the microhardness value, considering P value was below 0.10 for all conditions in a 90% confidence interval. The ANOVA classification determined that the substrate preheating control factor was the most influent factor on the measured microhardness, followed by powder particle size and feed rate. The spraying distance has less influence on the coating microhardness.

Figure 8 shows the influence of each parameter, indicating that the lowest level of hardness was reached when the powder had the smallest particle size. This fact is explained by considering that the smaller the particle size the greater the interface formation between the splats formed in the coating. On the other hand, the smaller

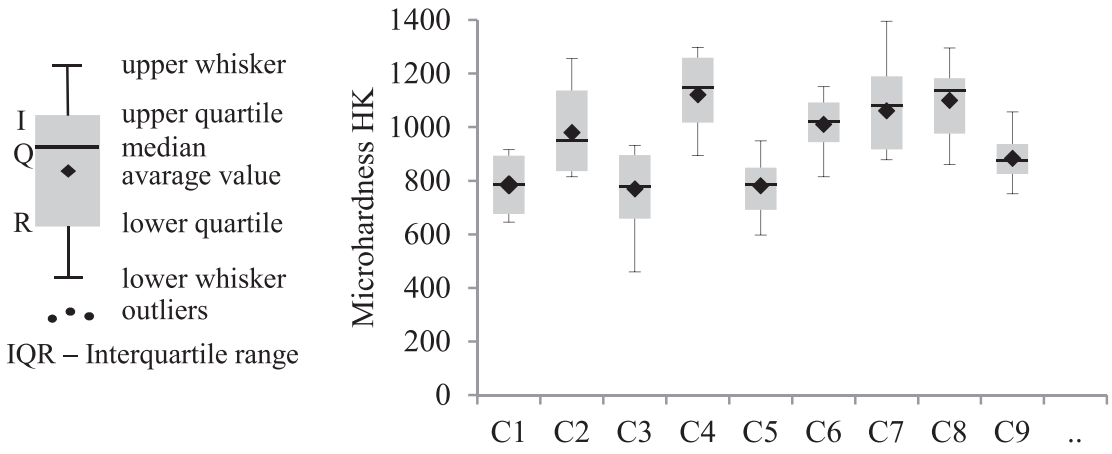

Figure 7. Coating's Knopp microhardness.

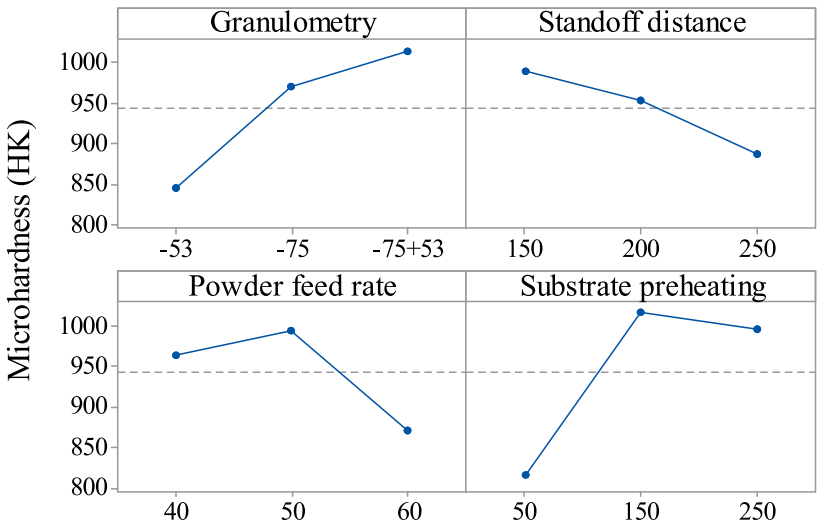

Figure 8. Main effects on the mean microhardness.

spraying distance increased the microhardness value, since particles that had a lower trajectory until reaching the substrate would be with a higher energetic level, and in this way would lead to the formation of a smaller amount of porosity, and consequently better cohesion between splats. It was evidenced that the feed rate had no great influence on the coating microhardness.

3.3. Electrochemical characterization

Corrosion resistance is an important characteristic for coatings. Interface plays a very important role; this region must have galvanic compatibility, adhesion and high density to prevent the contact of the substrate to the corrosive media. On the other hand, the minimum thickness of the coating is a fundamental requirement to ensure the corrosion resistance, since such a premise would prevent corrosive agents from penetrating the coating towards the substrate through the interconnected porosity [44].

The open circuit potential (OCP) measurements are shown in figure 9. It can be observed in the OCP curves that the FeNbC coatings shift the OCP to less active potentials when compared with the uncoated steel, demonstrating a better behavior of the coated systems compared to the steel without coating, in terms of protection to the substrate against corrosion. Additionally, it can be seen that the process parameters have influence on the coatings corrosion behavior related to the different compositions and microstructure produced. The existence of punctual defects on the coating promotes a corrosion intensification due to the formation of electrolytic cells between the small anode areas constituted by the discontinuities present in the coating and a large cathode area formed by the coating itself.

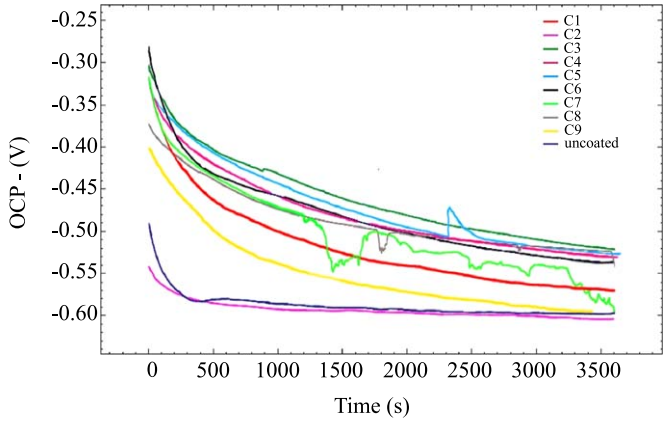

Figure 9. OCP curves for the coating and substrate.

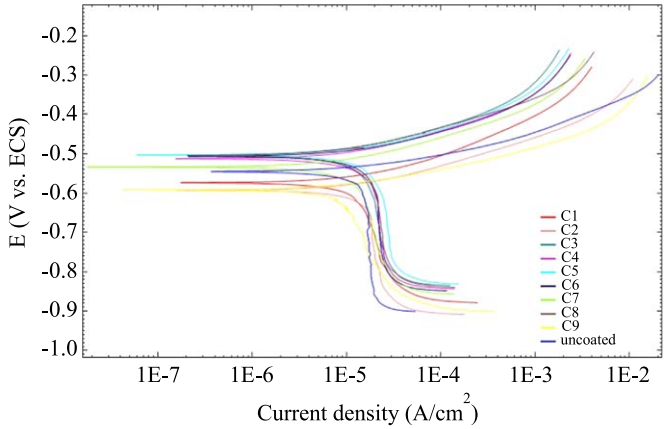

Figure 10. Polarization curves for the coating and substrate.

Table 4. Electrochemical parameters in 3.5% NaCl solution for FeNbC coating and non-coated steel obtained by Tafel linear extrapolation method.

Experimental condition	i_{corr} (μA cm^{-2})	E_{corr} (mV)	R_p (Ω cm^{-2})
C1	1.14	−573	2197
C2	2.64	−591	1800
C3	1.36	−502	3036
C4	1.65	−512	2505
C5	2.21	−502	1925
C6	2.47	−506	1886
C7	1.36	−533	3036
C8	1.22	−504	2723
C9	1.80	−590	2702
Substrate	1.88	−545	1534

Figure 10 shows the polarization curves for the FeNbC coatings deposited on the SAE/AISI 1020 substrate and its corrosion potential, polarization results for the uncoated substrate are also included for comparison purposes.

An apparent displacement of the cathodic and anodic branches was observed as a function of the coating composition when compared to the same curve of the uncoated sample. In addition, the cathodic curve exhibited a passivation region. The results obtained in the polarization tests indicate that the FeNbC coating in most cases improved electrochemical behavior compared to the uncoated sample, however this performance of

corrosion resistance could be differentiated. It is suggested that this behavior may be affected by low compaction and the presence of porosity and other defects such as voids and cracks in the coating, this condition was also related by other authors [45].

The table 4 presents the electrochemical parameters obtained by Tafel linear extrapolation method. The results indicate that FeNbC coatings, in general, tended to improve corrosion resistance of steel, since corrosion potential (E_{corr}) presented a less active potential values and a higher polarization resistance compared to uncoated steel, with the exception of experimental conditions 1, 2 and 9 that presented higher potential for active corrosion. These experimental conditions were those that presented higher levels of interlamellar oxides formed in the coating. Thus suggesting that the presence of oxides would induce regions of discontinuities in the microstructure of the coating and consequently affect the corrosion resistance.

4. Conclusion

The results obtained from XRD indicate that the FeNbC powder used to obtain thermal spraying coating was mainly composed of Fe and NbC rich phase, which were maintained after deposition.

The coating microstructure analysis by SEM images characterized the heterogeneity, by the presence of regions with visible porosity and voids, as well as interlamellar oxides, confirmed by chemical mapping analysis of EDS and XRD of the coating.

Coating microhardness presented an average value of 1084 HK, about 5 times higher than the value observed for SAE/AISI 1020 steel. This behavior could be associated to the presence of the niobium carbide in the matrix of iron and aluminum, as well as due to the coexistence of oxides originated in the flame spraying process.

In terms of corrosion resistance, the coating obtained in this study can promoted the reduction of the substrate corrosion rate, but this was not as significant due to the presence of porosity and voids, which compromised the corrosion barrier effect of the coating. The results obtained by potentiodynamic polarization curves and open circuit potential measurement also indicated the presence of discontinuities in FeNbC coating.

Acknowledgments

The authors would like to thank the CBMM (Companhia Brasileira de Metalurgia e Mineração) for the donation of research material and IFSC (Instituto Federal de Santa Catarina) for the granting of leave for training according to Ordinance No 1587/2016. The present study was carried out with the support of CAPES financing code 001. Thanks to FAPESC for financial support through the Project 2017TR 652.

ORCID iDs

I Bonetti https://orcid.org/0000-0003-0886-0163
E A dos S de https://orcid.org/0000-0002-1207-7078
J C G Milan https://orcid.org/0000-0001-7796-7605

References

[1] Departamento Nacional de Produção Mineral 1997 *Sumário. Mineral. Brasileiro* (Brasília: DNPM)
[2] Sá Brito V R S, Bastos I N and Costa H R M 2012 Corrosion resistance and characterization of metallic coatings deposited by thermal spray on carbon steel *Mater. Des.* **41** 282–8
[3] Majumdar S, Sengupta P, Kale G B and Sharma I G 2015 Development of multilayer oxidation resistant coating on niobium and tantalum *Surf. Coatings Technol.* **200** 3713–8
[4] Woydt M and Mohrbacher H 2015 The use of niobium carbide (NbC) as cutting tools and for wear resistant tribosystems *Int. J. Refract. Met. Hard Mater.* **49** 212–8
[5] Zhang L, Sun D and Yu H 2008 Effect of niobium on the microstructure and wear resistance of iron-based alloy coating produced by plasma cladding *Mater. Sci. Eng.* **490** 57–61
[6] Henderson D R 2016 Statistics overview *TANB* **164** 20–5 1019–2026
[7] Ray A and Bhadeshia H K D H 2015 Niobium in microalloyed rail steels *HSLA 2015, Microlloying 2015 and Offshore Engineering Steels, 2015* (https://doi.org/10.1007/978-3-319-48767-0)
[8] Bémont E, Cadel E, Maugis P and Blavette D 2004 Precipitation of niobium carbides in Fe–C–Nb steel *Surf Interface Anal.* **36** 585–8
[9] Petrikowski K, Fenker M, Gäbler J, Hagemann A, Pleger S and Schäfer L 2013 Study of CrNx and NbC interlayers for HFCVD diamond deposition onto WC-Co substrates *Diam. Relat. Mater.* **33** 38–44
[10] Saruki K, Hotta S, Fujita H and Arai T 1989 Fatigue strength of steels with thin *Thin Solid Films.* **181** 383–95
[11] Koropchak J A and Roychowdhury S B 1990 Evidence for aerosol ionic redistribution within aerosols produced by chrome electroplating *Environ. Sci. Technol.* **24** 1861–3
[12] Vardelle A *et al* 2016 The 2016 thermal spray roadmap *J. Therm. Spray Technol.* **25** 1376–440

[13] Pombo R R M H, Paredes R S C, Wido S H and Calixto A 2007 Comparison of aluminum coatings deposited by flame spray and by electric arc spray *Surf. Coatings Technol.* **202** 172–9
[14] Chaliampalias D *et al* 2013 Formation and oxidation resistance of Al/Ni coatings on low carbon steel by flame spray *Surf. Coat Technol.* **255** 5–11
[15] Young R M and Pfender E 1985 Generation and behavior of fine particles in thermal plasmas-A review *Plasma Chem Plasma Process.* **5** 1–37
[16] Sucharski G B, Geraldo A, Pukasiewicz M and Váz R F 2015 Optimization of the Deposition Parameters of HVOF FeMnCrSi+Ni+B Thermally Sprayed *Coatings Soldag e Inspeção.* **20** 238–52
[17] Li C J and Yang G J 2013 Relationships between feedstock structure, particle parameter, coating deposition, microstructure and properties for thermally sprayed conventional and nanostructured WC-Co *Int J. Refract. Met. Hard Mater.* **39** 2–17
[18] Berger L-M 2007 Hardmetals as thermal spray coatings *Powder Metall.* **50** 205–14
[19] Yan J, Liu L, Mao Z, Xu H and Wang Y 2014 Effect of spraying powders size on the microstructure, bonding strength, and microhardness of $MoSi_2$ coating prepared by air plasma spraying *J. Therm. Spray Technol.* **23** 934–9
[20] Sudha C, Shankar P, Rao R V S, Thirumurugesan R, Vijayalakshmi M and Raj B 2008 Microchemical and microstructural studies in a PTA weld overlay of Ni-Cr-Si-B alloy on AISI 304L stainless steel *Surf Coatings Technol.* **202** 2103–12
[21] Bourithis L, Milonas A and Papadimitriou G D 2003 Plasma transferred arc surface alloying of a construction steel to produce a metal matrix composite tool steel with TiC as reinforcing particles *Surf. Coatings Technol.* **165** 286–95
[22] Paredes R S C, Amico S C and d'Oliveira A S C M 2006 The effect of roughness and pre-heating of the substrate on the morphology of aluminium coatings deposited by thermal spraying *Surf. Coatings Technol.* **200** 3049–55
[23] González R, Cadenas M, Fernández R, Cortizo J L and Rodríguez E Wear behaviour of flame sprayed NiCrBSi coating remelted by flame or by laser *Wear* **262** 301–7
[24] Duarte L T, Paula E M, Silva E, Branco J R T and Lins V F C Production and characterization of thermally sprayed polyethylene terephthalate coatings *Surf. Coatings Technol.* **182** 261–7
[25] Uyulgan B *et al* 2007 Wear behaviour of thermal flame sprayed FeCr coatings on plain carbon steel substrate *J Mater Process Technol.* **190** 204–10
[26] Yao J T, Ren J Q, Bin H H, Yang G J, Li C X and Li C J 2014 Deposition behavior of semi-molten spray particles during flame spraying of porous metal alloy *J. Therm. Spray Technol.* **23** 991–9
[27] Redjdal O, Zaid B, Tabti M S, Henda K and Lacaze P C 2013 Characterization of thermal flame sprayed coatings prepared from FeCr mechanically milled powder *J. Mater. Process Technol.* **213** 779–90
[28] Jr T R C 1993 Thermal spray coatings *Handb Surf. Eng.* **5** 1446–71
[29] Yang K, Fukumoto M, Yasui T and Yamada M 2010 Study of substrate preheating on flattening behavior of thermal-sprayed copper particles *J. Therm. Spray Technol.* **19** 1195–205
[30] Yadav A K, Arora N and Dwivedi D K 2006 On microstructure, hardness and wear behaviour of flame sprayed Co base alloy coating deposited on mild steel *Surf. Eng.* **22** 331–7
[31] Bianchi L, Denoirjean A, Blein F and Fauchais P 1997 Microstructural investigation of plasma-sprayed ceramic splats *Thin Solid Films.* **299** 125–35
[32] Fauchais P, Montavon G and Bertrand G 2010 From powders to thermally sprayed coatings *J. Therm. Spray Technol.* **19** 56–80
[33] Torres B, Rodrigo P, Campo M, Ureña A and Rams J 2009 Oxy-acetylene flame thermal spray of Al/SiC p composites with high fraction of reinforcements *J. Therm. Spray Technol.* **18** 642–51
[34] Fauchais P and Vardelle A 2012 Thermal sprayed coatings used against corrosion and corrosive wear *Advanced Plasma Spray Applications* ed H S Jazi (In Tech) 3–39
[35] Mellali M, Fauchais P and Grimaud A 1996 Influence of substrate roughness and temperature on the adhesion/cohesion of alumina coatings. *Surf Coatings Technol* **95** 02540
[36] Cruz E B and Fridman D P 2018 Development of FeNbC for wear resistant applications *Int. Symp. on Wear Resistant Alloys fot the Mining and Processing Industry* 978-0-692-05382-9
[37] Koch C C and Whittenberge J D 1996 Mechanical milling / alloying of intermetallics *Intermetallics* **4** 339–55
[38] Özdemirler D, Gündüz S and Erden M A 2017 Influence of NbC addition on the sintering behaviour of medium carbon PM steels *Metals (Basel).* **7** 1–11
[39] Deshpande S, Sampath S and Zhang H 2006 Mechanisms of oxidation and its role in microstructural evolution of metallic thermal spray coatings—Case study for Ni-Al *Surf Coatings Technol.* **200** 5395–406
[40] Dussoubs B, Vardelle A, Mariaux G, Themelis N J and Fauchais P 2001 Modeling of plasma spraying of two powders *Therm. Spray Technol.* **10** 105–10
[41] Brandolt C, de S, Souza J G Jr, de, Kunst S R, Vega M R O, Schroeder R M and Malfatti C de F 2014 Niobium and niobium-iron coatings on API 5LX 70 steel applied with HVOF *Mater Res.* **17** 866–77
[42] Mao W G *et al* 2012 Evaluation of microhardness, fracture toughness and residual stress in a thermal barrier coating system: a modified Vickers indentation technique *Surf Coatings Technol.* **206** 4455–61
[43] Yu H L, Zhang W, Wang H M, Yin Y L, Ji X C and Zhou K B 2016 Comparison of surface and cross-sectional micro-nano mechanical properties of flame sprayed NiCrBSi coating *J Alloys Compd.* **672** 137–46
[44] Vackel A, Dwivedi G and Sampath S 2015 Structurally integrated, damage-tolerant, thermal spray coatings *Miner Met Mater Soc.* **67** 1540–53
[45] Silva A, de S, Martinelli A E, Scatena H Jr, Silva J H E, Alves C Jr and Távora M P Electrochemical behavior of steel-FeNbC composites used in the production of oxygen *Mater Res.* **8** 151–3